J.Korean Asso. Radiat. Prot.
Vol.23 No.3 : 175-184(1998)

■技術論文■

# Analysis of Dose Rates from Steam Generators to be Replaced from Kori Unit 1

**Sang-Woon Shin, Jung-Kwon Son, Chan-Hee Cho and Myung-Jae Song**
*Korea Electric Power Research Institute*
*103-16 Munji-Dong, Yusong-Ku, Taejon, 305-380, Korea*

# 고리 1호기 교체 증기발생기의 선량률 분석

**신상운 · 손중권 · 조찬희 · 송명재**
전력연구원

(1998년 7월 1일 접수, 1998년 11월 7일 채택)

**Abstract** - In order to calculate dose rates from steam generators to be replaced from Kori unit 1 in 1998, radionuclide inventories inside steam generator were evaluated from smear test results and measured dose rates from S/G tubes withdrawn for the metallographical examination of damaged tubes. Based on the inventories, contact dose rates and dose rates at 1 m from the surface of a steam generator were calculated using the QAD-CG computer code. Contact dose rates ranged from 11.5 mR/hr at the bottom of channel head to 37.7 mR/hr at the middle of shell barrel, and showed no significant difference with dose rates at 1 m from the surface of steam generator. Shielding effects of lead and carbon steel were compared to provide basic shielding data. Lead shield showed excellent shielding effects. Dose rate at 1 m from the middle of S/G shell barrel decreased from 38.6 mR/hr to 15.5 mR/hr with the lead shield of 2 mm thickness. However, carbon steel showed a poor shielding effect even with the thickness of 2.0 cm. This can be explained with the great differences in the attenuation effect and buildup factor between lead and carbon steel for low energy photons.
*Key Words : Dose Rate, Shielding Calculation, Steam Generator, QAD-CG, Contamination*

**요약** - 1998년에 고리 1호기로부터 교체될 증기발생기의 선량율을 계산하기 위하여 Smear 오염검사 결과와 튜브 손상원인을 규명하기 위하여 인출하였던 증기발생기 튜브의 선량율 측정결과로부터 증기발생기 내부의 방사성핵종 재고량을 평가하였다. 방사성 핵종 재고량을 토대로 QAD-CG 컴퓨터 코드를 이용하여 증기발생기 표면의 접촉 선량율과 1 m 이격 선량율을 계산하였는데, 접촉 선량율은 Channel Head의 하부에서 최저인 11.5 mR/hr를 나타냈으며, Shell Barrel의 중간 지점에서 최대값인 37.7 mR/hr를 나타냈다. 한편 접촉 선량율과 1 m 이격 선량율은 증기발생기의 크기로 인해 큰 차이를 보이지 않았다. 또한 증기발생기의 차폐가 필요할 경우 요구되는 기본적인 데이터를 마련하기 위하여 납과 탄소강의 차폐 특성을 비교해 보았다. 납을 차폐체로 사용할 경우 2 mm 두께만으로도 증기발생기 Shell Barrel 중간 지점에서의 표면 선량율이 37.7 mR/hr에서 15.7 mR/hr로 감소되었다. 그러나 탄소강의 경우에는 차폐체의 두께를 2 cm로 증가시킨다고 하더라도 차폐효과가 매우 낮았다. 이러한 차폐효과 차이는 저에너지 광자에 대한 납과 탄소강의 감쇄효과 차이와 축적인자 차이 때문에 발생되는 것으로 추정된다.

## INTRODUCTION

Kori unit 1 has planned to replace old steam generators with new ones. The steam generators to be replaced will be conditioned to prevent the spread of contamination after isolating them from the primary coolant system using a mechanical cutting technique. Then they will be transported from the containment building to the radwaste storage building which is located in the same site. Therefore, it is not necessary to meet the legal requirements for transportation of radioactive materials which are applied when transporting radioactive materials from a site to the other site.

However, dose rates from the steam generators to be replaced are very important for planning jobs related to the replacement of steam generators and the transportation of the replaced steam generators. In addition, the shielding condition for the transport of the steam generators to the other site may be prepared for the worst case.

In this paper, radionuclide inventory inside steam generators was evaluated based on the smear test results, and measured and calculated dose rates from S/G tubes withdrawn for the metallographical examination of damaged tubes. Then, dose rates from the steam generators to be replaced were evaluated using the QAD-CG computer code[1] to provide preliminary data for planning jobs related to the replacement of them. Shielding effect was also analyzed for lead and carbon steel.

## RADIONUCLIDE INVENTORY PREPARATION

In order to calculate dose rates from the steam generators to be replaced, inventory and distribution of radioactivity inside the steam generator at the time of transportation should be known.

Two sets of measured data are available. One relates smear test results for crud deposited in the S/G chamber, which provides a valuable information on the radionuclide composition of contaminants. The other relates measured dose rates from the tubes withdrawn for the metallographical examination of damaged tubes. If the composition of radionuclides inside S/G tubes is known, the surface concentration inside the tubes can be determined approximately from the measured dose rates.

The surface concentration inside the chamber was evaluated from the smear test results by assuming that the detection efficiency of smear test is 1%. The detection efficiency of 1% seems to be quite conservative. The effect of uncertainty involved in the detection efficiency will be discussed later. Then total radionuclide inventory in the chamber can be calculated from the surface concentration and total surface area

**Table 1.** Surface Contamination inside S/G Chambers Measured with Smear Test Method.

(Unit: kBq/100 cm$^2$)

| Nuclide | S/G A | | S/G B | | Average Portion %) |
|---|---|---|---|---|---|
| | Hot Leg | Cold Leg | Hot Leg | Cold Leg | |
| Cr-51 | 7.52E-01 | 8.16E-01 | 2.98E-00 | - | 4.42 |
| Mn-54 | 5.28E-01 | 3.51E-01 | 3.94E-01 | - | 1.24 |
| Fe-59 | 2.90E-01 | 1.10E-01 | 3.80E-01 | - | 0.76 |
| Co-57 | 5.95E-02 | 5.14E-02 | - | - | 0.11 |
| Co-58 | 1.06E+01 | 1.10E+01 | 8.35E-00 | 6.95E-00 | 35.86 |
| Co-60 | 5.65E-00 | 6.38E-00 | 4.95E-00 | 6.80E-00 | 23.11 |
| Zn-65 | 3.33E-01 | 3.76E-01 | - | - | 0.69 |
| Sr-85 | 8.28E-01 | 8.52E-01 | 7.52E-01 | 2.43E-00 | 4.72 |
| Zr-95 | 2.32E-01 | - | 1.84E-00 | - | 2.01 |
| Nb-95 | 3.80E-01 | 3.43E-01 | 2.82E-00 | - | 3.44 |
| Ru-103 | 5.76E-01 | 2.62E-01 | 4.84E-00 | - | 5.51 |
| Ru-106 | - | - | 6.78E-00 | - | 6.59 |
| Sn-113 | - | - | 1.96E-01 | - | 0.19 |
| Cs-136 | 1.27E-01 | 5.16E-01 | 9.51E-02 | 8.47E-00 | 8.94 |
| Ce-141 | 1.92E-01 | 8.23E-02 | 8.13E-01 | - | 1.06 |
| Ce-144 | - | - | 1.39E-00 | - | 1.35 |
| Total | 20.7 | 21.1 | 36.6 | 24.6 | 100.0 |

Table 2. Radionuclide Composition of Crud Deposited onto the Surfaces of S/G Tubes.

| Nuclide | Radionuclide Composition at Shutdown (%) |
|---|---|
| Cr-51 | 13.90 |
| Mn-54 | 1.42 |
| Fe-59 | 1.57 |
| Co-57 | 0.13 |
| Co-58 | 57.63 |
| Co-60 | 24.54 |
| Zn-65 | 0.81 |

inside the chamber. Table 1 shows the smear test results carried out at 44 days after shutdown in 1997. Average radionuclide composition and the maximum smear test results found in the hot leg side of S/G B were used to calculate the surface radionuclide concentration inside the chamber at the time of shutdown.

Surface concentration of each nuclide at the time of measurement was corrected for decay during the elapsed time after shutdown to obtain surface concentration at the time of shutdown. Inventory of each nuclide inside the chamber can be calculated from the surface radionuclide concentration at the time of shutdown and the surface area of 336,031 $cm^2$ evaluated from the S/G design specifications[3]. The resulted total radioactivity inside the chamber was estimated as $2.82 \times 10^4$ MBq at the time of shutdown.

In order to decide radionuclide inventory in the tube region, the radionuclide composition of crud deposited in the primary side of S/G tubing was determined from the radionuclide composition found in the crud sampled from the surface of the chamber. In general, it is expected that the tube crud has similar composition to the chamber crud. However, there are several important factors to be considered, which can affect the deposition mechanism of crud into the surfaces of the chamber and the tubes. One is the difference in the materials. The tubes are made of Inconel-600, whereas the chambers are made of stainless steel. Deposition rate and release rate of crud depend on the type of base material[8]. Roughness of the surface is also different for the chamber and the tubes. Deposition rate onto the smooth surface of tubes must be lower than that onto the rough surface of chamber. Vertical direction of tubes can cause small deposition of particles onto their surface compared to the chamber surface. Considering these differences, we assumed that ionic deposition is dominant in case of S/G tubes. That is, only activated corrosion products, which are generally re-deposited onto the surfaces of out-core components through ionic deposition process after being activated in the core, were assumed to be deposited onto the tube surface. Then the radionuclide composition of tube crud can be evaluated from that of chamber crud by assuming that the composition of corrosion products is identical for both of them.

Table 2 shows the radionuclide composition of tube crud evaluated from the data given at the time of shutdown. Even though there must be some other fission products in the tube crud, most of them has short half-life, and emit low energy photons. Therefore, the effect of those nuclides on the dose rate from the surface of steam generator is not so great compared to that of Co-60. It is reported that Co-60 and Co-58 are major radiation sources in the nuclear power plant[2]. No significant error in the dose rate will be resulted from the assumption of radionuclide composition given in Table 3.

Surface concentration inside the tubes can be evaluated from the measured dose rate using the QAD-CG computer code. Four pieces of damaged tubes were sent to research organizations for the metallographical analysis of damaged tubes in order to examine the cause of tube failure. Prior to shipping of them, maximum contact dose rates were measured.

**Table 3.** Calculated Radionuclide Inventory inside S/G Chamber.

| Nuclide | Surface Contamination at Shutdown (kBq/cm$^2$) | Surface Contamination at Transportation (kBq/cm$^2$) | Total Inventory at Transportation (MBq) |
|---|---|---|---|
| Cr-51 | 4.86E-00 | 2.30E-00 | 7.71E+02 |
| Mn-54 | 4.99E-01 | 4.67E-01 | 1.57E+02 |
| Fe-59 | 5.50E-01 | 3.45E-01 | 1.16E+02 |
| Co-57 | 4.41E-02 | 4.09E-02 | 1.37E+01 |
| Co-58 | 2.02E+01 | 1.50E+01 | 5.05E+03 |
| Co-60 | 8.58E-00 | 8.49E-00 | 2.85E+03 |
| Zn-65 | 2.86E-01 | 2.62E-02 | 8.81E+01 |
| Sr-85 | 2.77E-00 | 2.01E-00 | 6.75E+02 |
| Zr-95 | 1.18E-00 | 8.55E-01 | 2.87E+02 |
| Nb-95 | 3.01E-00 | 1.66E-00 | 5.58E+02 |
| Ru-103 | 4.38E-00 | 2.58E-00 | 8.67E+02 |
| Ru-106 | 2.61E-00 | 2.47E-00 | 8.31E+02 |
| Sn-113 | 9.06E-02 | 7.56E-02 | 2.54E+01 |
| Cs-136 | 3.32E+01 | 6.84E-00 | 2.30E+03 |
| Ce-141 | 9.87E-01 | 5.21E-01 | 1.75E+02 |
| Ce-144 | 5.51E-01 | 5.11E-01 | 1.72E+02 |
| Total | 83.6 | 44.5 | 1.49E+04 |

Radionuclide composition at the time of shipping was calculated from the estimated inventory at the time of shutdown by adjusting radioactive decay during the elapsed time after shutdown. And maximum contact dose rate per unit surface concentration at the shipping point was evaluated using the QAD-CG computer code. Then, surface concentration inside the tubes, which gave the measured contact dose rate, was obtained. Again surface concentration of each radionuclide at the time of shutdown was calculated from the surface concentration at the shipping point.

Table 3 and 4 show the surface concentration of each radionuclide at the time of shutdown and at the time of transport of the steam generators to be replaced. The inventory of each nuclide is also given in Table 3 and 4.

## DOSE RATE ANALYSIS

Expected dose rates from the steam generators to be replaced at the time of transport to the radwaste storage building were calculated using the QAD-CG computer code. In order to prepare input data for the QAD-CG computer code, a steam generator was segmented into two regions, S/G chamber and S/G tubes. Transition cone region was excluded in the input geometry. In the region of chamber, it was assumed that radionuclides were present on the top of inner shell with the thickness of 1 mm. However, homogeneous mixture was assumed in the tube region. From the design specifications, the thickness of shell was assumed to 13.6 cm in the chamber, and 8 cm in the trunk[3]. Fig. 1 shows the S/G configuration used to prepare a QAD-CG input file.

Gamma flux was determined from the inventory of each nuclide given in Table 3 and 4, and gamma emission probability from each nuclide given in Ref. 4. Based on the gamma energies and their flux, it was divided into 6 groups in the tube region, and 7 groups in the chamber region. Then average energy was calculated for each energy group by weighting gamma flux.

Dose rate conversion factor for each energy group was calculated from the following equation[5].

$$C_x = \frac{(\mu_{en}/\rho)_{air}\, E}{1.5\times 10^4} \quad (1)$$

where $C_x$ : dose rate conversion factor (R cm$^2$

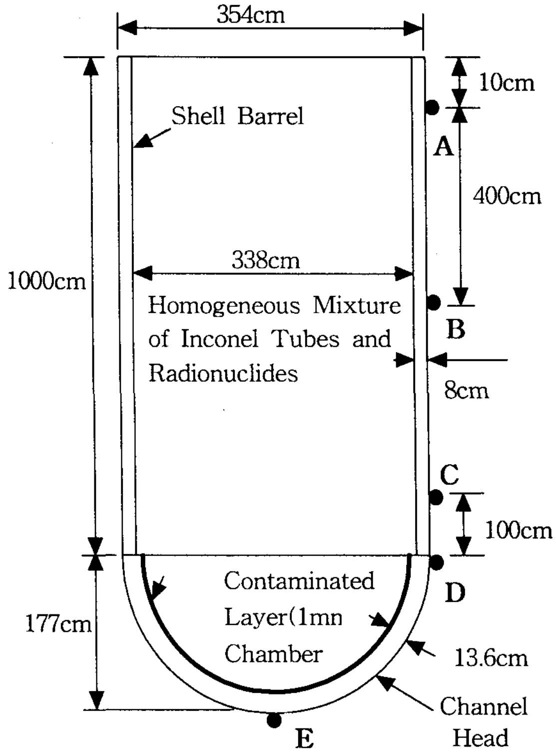


● : selectFive ed positions for the calculation of dose rates

**Fig. 1.** Simplified S/G Configuration for the Analysis of Dose Rates

sec/h)

$(\mu_{en}/\rho)_{air}$ : mass energy absorption coefficient for a $E$ MeV photon in air

Five positions, which are 1 m from the upper part of shell barrel, the middle of shell barrel, 1 m from the lower part of shell barrel, the upper part of channel head, and the bottom of channel head, were selected for the analysis of contact dose rates and dose rates at 1 m from the surface of steam generator. Selected positions are designated as *A*, *B*, *C*, *D*, and *E* in Fig. 1, respectively. An input file for QAD-CG prepared for the calculation of dose rate from the contamination in tube region was given in Table 5.

Table 6 shows dose rates calculated with the QAD-CG computer code for the five selected positions. The highest contact dose rate of 37.7 mR/hr was found in the middle of shell barrel, and the lowest contact dose rate of 11.5 mR/hr was found in the center of channel head. As shown in the Table, there is no significant difference between contact dose rates and 1 m dose rates. What is more, the 1 m dose rate is higher than the contact dose rate at the middle of shell barrel. This is because of large geometry of steam generator. In particular, difference in the penetrating thickness of photons emitted from the upper and lower parts of the tube region makes the 1 m dose rate even higher than the contact dose rate at the middle of shell barrel.

It is noteworthy that the dose rates due to the surface contamination inside the chamber is negligible compared to the dose rates due to the contamination in the tube region. Surface concentration was determined from the assumed detection efficiency of smear test method. Detection efficiency of smear test method is not reported. An experienced technician informed that it ranged from 5 to 50% in his experiment depending on the type of contamination. However, the experiment was carried out on the smooth surface. Therefore, it is expected that the detection efficiency of smear test method used to determine surface contamination on the rough inner surface of S/G chamber is far below 5%. If the detection efficiency was less than 1% which was assumed here, the surface radionuclide concentrations inside the chamber must have been underestimated. Thus the effect of possible underestimation of surface contamination should be addressed. From Table 6, the highest contact dose rate from the chamber contamination is only 0.12 mR/hr, which is less than 1% of corresponding dose rate from the tube contamination. It implies that uncertainty involved in the assumed detection efficiency has meaningless effect on the calculated dose rates given in Table 6.

Heterogeneous distribution of radioactivity in the tube region can cause considerable error in the calculated dose rates. In case of S/G A, for example, measured contact dose rate at the lower part of shell barrel was about two times higher than that at the middle of shell barrel as shown in Table 7[6]. This is probably because of high contamination in the tubesheet region. The possibility of high contamination in the U-tube region should be also considered. Such a

**Table 5.** An Example of QAD-CG Input File for the Calculation of Dose Rate from Tubesheet Contamination.

```
S/G Dose Rate Analysis from Tubeside Contamination

  10  20  20   11   3   1   6    0   0    5   1    0  1000 4000 1000 0
 3.312E12  0.      0.      0.       0.      0.      0.
0.0      16.9     33.8     50.7     67.6     84.5     101.4    118.3
135.2    152.1    169.0
0.0      50.0     100.0    150.0    200.0    250.0    300.0    350.0
400.0    450.0    500.0    550.0    600.0    650.0    700.0    750.0
800.0    850.0    900.0    950.0    1000.0
0         0.3142   0.6283   0.9425   1.2566   1.5708   1.8850   2.1991
2.5133   2.8274   3.1416   3.4558   3.7699   4.0841   4.3982   4.7124
5.0266   5.3407   5.6549   5.9690   6.2832
   0     0              QAD-CG S/G Dose Rate Analysis
  RPP  1  -500.0     500.0     -500.0     500.0      -500.0     1000.0
  SPH  2  0.         0.         0.        163.4
  SPH  3  0.         0.         0.        177.0
  RCC  4  0.         0.         0.        0.         0.         1000.0
          169.0
  RCC  5  0.         0.         0.        0.         0.         1000.0
          177.0
  END
  AR1     2       2        -4
  CSH     3       3        -2         -5
  TSO     3       4
  TSH     3       5        -4
  AR3     2       1        -3         -5
  END
    1     1     1     1     1
    1     2     3     2     1
    3    6     7    8    14   15    16   24    25   26    28   42
      0.   9.56E-4   2.94E-4       0.        0.        0.        0.        0.
      0.       0.       0.
   0.0196      0.       0.     0.0236    0.0027    0.0031        0.    0.1021
   7.6420   0.0432   0.0393
      0.        0.       0.        0.        0.        0.   8.45E-2        0.
  3.70E-2   0.4067      0.
    0.15      0.32      0.51      0.82      1.17      1.33
 1.936E-3 8.385E-3 1.669E-1 5.777E-1 3.226E-1 3.209E-1
 2.481E-4 6.126E-4 1.005E-3 1.567E-3 2.103E-3 2.321E-3
      1.0       1.0       1.0       1.0       1.0       1.0       1.0
    0.1-1.4
    0.1-0.2      0.2-0.4      0.4-0.6      0.6-1.0      1.0-1.2      1.2-1.4
mev/cm*2-sec                mrem/hr                        w/g
        0.    -177.1      0.     1    0    0    0
        0.    -277.       0.     1    0    0    0
        0.    -377.       0.     1    0    0    0
        0.    -477.       0.     1    0    0    0
        0.       0.     177.1    1    0    0    0
        0.       0.     277.     1    0    0    0
        0.       0.     377.     1    0    0    0
        0.       0.     477.     1    0    0    0
        0.     100.     177.0    1    0    0    0
        0.     100.     277.     1    0    0    0
        0.     100.     377.     1    0    0    0
        0.     100.     477.     1    0    0    0
        0.     500.     177.1    1    0    0    0
        0.     500.     277.     1    0    0    0
        0.     500.     377.     1    0    0    0
        0.     500.     477.     1    0    0    0
        0.     900.     177.1    1    0    0    0
        0.     900.     277.     1    0    0    0
        0.     900.     377.     1    0    0    0
        0.     900.     477.     1    0    0    0
        0.     -20.       0.0    1    0    0    0
        0        0        0     -1    0    0    0
```

**Table 6.** Analysis Result of Dose Rates from Steam Generator Using the QAD-CG Computer Code.

(Unit: mR/hr)

| | | Chamber Contamination | Tube Contamination | Total |
|---|---|---|---|---|
| Surface Contamination (kBq/cm²) | | 44.5 | 69.21 | |
| Total Inventory (MBq) | | 1.49E+04 | 3.31E+06 | 3.33E+06 |
| Upper Part of Shell Barrel (*A*) | Contact Dose Rate | 0.0075 | 29.8 | 29.8 |
| | 1 m Dose Rate | 0.0071 | 30.8 | 30.8 |
| Middle of Shell Barrel (*B*) | Contact Dose Rate | 0.023 | 37.7 | 37.7 |
| | 1 m Dose Rate | 0.019 | 38.6 | 38.6 |
| Lower Part of Shell Barrel (*C*) | Contact Dose Rate | 0.12 | 25.8 | 25.9 |
| | 1 m Dose Rate | 0.054 | 23.9 | 24.0 |
| Upper Part of Channel Head (*D*) | Contact Dose Rate | 0.12 | 14.3 | 14.4 |
| | 1 m Dose Rate | 0.087 | 11.1 | 11.2 |
| Bottom of Channel Head (*E*) | Contact Dose Rate | 0.025 | 11.5 | 11.5 |
| | 1 m Dose Rate | 0.11 | 5.1 | 5.2 |
| Inside S/G Chamber | | 117 | 5,084 | 5,201 |

high contamination in the U-tube region can cause high dose rates in the transition cone area. Therefore, possible heterogeneous distribution of radioactivity in the tube region should be considered for shielding purpose.

In the tube region, tubes are opened to S/G chamber region. Such openings can serve as direct paths of gamma rays emitted from the inner tube surfaces. These direct penetrations increase the dose rate inside the chamber. Therefore, such a homogeneous geometry in the tube region may cause underestimation of dose rate inside the chamber. The calculated dose rate inside the chamber was about 5.2 R/hr, which was half as much as the measured dose rate.[6] It should be noted that dose rates outside channel head may be higher than the calculated dose rates by a factor of ~2 because of the opening effect and the local high contamination.

## SHIELDING CALCULATION

The calculated dose rates at 1 m from the bare surface of steam generator exceeded 10 mR/hr. Therefore, in order to transport the steam generators to be replaced to the other site, they should be shielded in proper ways to reduce 1 m dose rates from the surfaces less than 10 mR/hr. For the comparison of shielding effects of different materials, lead and carbon steel are selected. Again, the QAD-CG computer code was used to calculate dose rates when shielding the replaced steam generators.

Table 8 summarizes the shielding effect of lead. As shown in Table 8, even 2 mm lead shield reduces the dose rates to about one-third of bare dose rates. Considering that the half value layer of lead is about 1 cm for 1 MeV photon, the result seems to be quite exceptional.

**Table 7.** Comparison between Calculated Dose Rates and Measured Dose Rates.

(Unit : mR/hr)

| Position | Calculated Contact Dose Rate | Measured Contact Dose Rate | |
|---|---|---|---|
| | | S/G A | S/G B |
| Upper Part of Shell Barrel (*A*) | 29.8 | 35 | 20 |
| Middle of Shell Barrel (*B*) | 37.7 | 35-50 | 30 |
| Lower Part of Shell Barrel (*C*) | 25.9 | 80 | 15-40 |
| Inside S/G Chamber | 5,201 | 10,000-11,000 | 11,000-13,000 |

**Table 8.** Shielding Effects of Lead on the S/G Dose Rates.

(Unit: mR/hr)

| Thickness of Lead (mm) | | 0 | 2 | 4 | 10 |
|---|---|---|---|---|---|
| Bottom of Channel Head | Contact | 11.5 | 3.6 | 3.1 | 2.1 |
| | 1 m | 5.2 | 1.5 | 1.4 | 0.9 |
| | 2 m | 2.8 | 0.8 | 0.7 | 0.5 |
| | 3 m | 1.8 | 0.5 | 0.5 | 0.3 |
| Lower Part of Shell Barrel | Contact | 25.8 | 7.8 | 6.6 | 4.3 |
| | 1 m | 24.0 | 7.9 | 6.8 | 4.4 |
| | 2 m | 15.2 | 5.0 | 4.3 | 2.8 |
| | 3 m | 11.1 | 3.6 | 3.1 | 2.1 |
| Middle of Shell Barrel | Contact | 37.7 | 15.7 | 13.6 | 8.7 |
| | 1 m | 38.6 | 15.5 | 13.3 | 8.5 |
| | 2 m | 27.9 | 11.1 | 9.5 | 5.9 |
| | 3 m | 21.3 | 8.3 | 7.1 | 4.3 |
| Upper Part of Shell Barrel | Contact | 29.8 | 10.9 | 8.7 | 5.6 |
| | 1 m | 30.8 | 11.2 | 9.7 | 6.3 |
| | 2 m | 20.1 | 7.5 | 6.5 | 4.3 |
| | 3 m | 14.7 | 5.6 | 4.8 | 3.1 |

**Table 9.** Shielding Effects of Carbon Steel on the S/G Dose Rates.

(Unit: mR/hr)

| Thickness of Carbon Steel (mm) | | 0 | 5 | 10 | 20 |
|---|---|---|---|---|---|
| Bottom of Channel Head | Contact | 11.5 | 9.4 | 6.3 | 5.1 |
| | 1 m | 5.2 | 4.1 | 2.8 | 2.2 |
| | 2 m | 2.8 | 2.3 | 1.5 | 1.3 |
| | 3 m | 1.8 | 1.4 | 1.0 | 0.8 |
| Lower Part of Shell Barrel | Contact | 25.8 | 23.2 | 19.4 | 18.2 |
| | 1 m | 24.0 | 22.6 | 20.9 | 20.1 |
| | 2 m | 15.2 | 14.5 | 13.6 | 13.2 |
| | 3 m | 11.1 | 10.7 | 10.1 | 9.9 |
| Middle of Shell Barrel | Contact | 37.7 | 36.9 | 35.3 | 34.6 |
| | 1 m | 38.6 | 37.4 | 35.5 | 34.6 |
| | 2 m | 27.9 | 27.0 | 25.4 | 24.7 |
| | 3 m | 21.3 | 20.6 | 19.3 | 18.7 |
| Upper Part of Shell Barrel | Contact | 29.8 | 29.8 | 29.9 | 29.9 |
| | 1 m | 30.8 | 30.4 | 29.9 | 29.5 |
| | 2 m | 20.1 | 19.8 | 19.3 | 19.0 |
| | 3 m | 14.7 | 14.4 | 13.9 | 13.7 |

However, further increase in the thickness of lead shield from 2 mm to 1 cm resulted in no more than 45% decrease in the dose rates.

From these findings, it is possible to judge that most gamma components contributing dose rates from the steam generators are composed of low energy photons. While penetrating the large thickness of S/G shell, high energy photons seem to lose their energy. For low energy photons, lead is a very effective shield. For example, the half value layer of lead shield is only 0.86 mm for X-rays with average energy of 250 keV[2]. Therefore, only 2 mm lead shield can reduce the dose rate from the X-ray source up to one-fifth of original dose rate.

No further dramatic decrease in the dose rate with the increase of lead shield thickness from 2 mm to 1 cm suggests that about one-third of gamma components are composed of high energy photons, which are mostly emitted from

Co-60 source in the vicinity of the shell.

Therefore, it is not a good way to increase the thickness of lead shield more than 2 mm when shielding steam generators with lead. Instead, increase of package sizing seems to be very effective.

As shown in Table 8, for example, the dose rates at 3 m from the surfaces of 2 mm shield were almost the same as the dose rates at 1 m from the surfaces of 1 cm shield.

Unlike the case of lead, carbon steel showed poor performance as a shield. Table 9 shows dose rates from steam generator when shielding the steam generator with carbon steel. As shown in Table 9, the shielding effect of carbon steel shows strong dependence on the position. It implies that energy spectrum of photons varies greatly with the position. Poor shielding performance of carbon steel can be explained with great difference in the half value layers for photons of energies from 200 keV to 500 keV between carbon steel and lead. In addition, carbon steel has large buildup factors compared to lead. For 500 keV photons, the buildup factor of iron is about three times higher than that of lead when $\mu x$ (relaxation length) is 4[7]. Because of its small attenuation and high dose buildup, carbon steel is not desirable as a shielding material of the replaced steam generators.

## CONCLUSION

Kori unit 1 will replace old steam generators with new ones in 1998. The steam generators to be replaced will be stored in the radwaste storage building located in the same site. Therefore, it is not necessary to meet the legal requirements for transportation of radioactive materials. However, dose rates from the steam generators to be replaced should be provided for the planning of jobs related to the replacement of steam generators and the transportation of the replaced steam generators. In addition, the shielding condition for the transport of the steam generators to be replaced to the other site may be prepared for the worst case.

In order to calculate dose rates from the replaced steam generators, radionuclide inventories inside steam generator were evaluated from smear test results and measured dose rates from S/G tubes withdrawn for the metallographical examination of damaged tubes. Total activity within a steam generator was about $3.3 \times 10^6$ MBq, and more than 99% of that was appeared to be present in the primary side of S/G tubing.

Contact dose rates and dose rates at 1 m from the surface of a steam generator were calculated using the QAD-CG computer code. Contact dose rates ranged from 11.5 mR/hr at the bottom of channel head to 37.7 mR/hr at the middle of shell barrel, and showed no significant difference with dose rates at 1 m, which were 5.2 and 38.6 mR/hr at the corresponding positions, respectively.

In order to provide optimum shielding condition for the transport of the steam generators, shielding effects for lead and carbon steel were analyzed. Lead shield showed excellent shielding effect. Dose rate at 1 m from the middle of S/G shell barrel decreased from 38.6 mR/hr to 15.5 mR/hr with the lead shield of 2 mm thickness. However, no further dramatic decrease in the dose rate was found even with the increase of lead shield thickness from 2 mm to 1 cm. It suggested that photons emitted from the surface of S/G might be grouped in two components, i. e., low energy component and high energy component. The low energy gamma component with the energy less than 500 keV can be attenuated very effectively with the small thickness of lead. On the contrast, carbon steel showed a poor shielding effect even with the thickness of 2.0 cm. This can be explained with the great differences in the attenuation effect and buildup factor between lead and carbon steel for low energy photons.

## REFERENCES

1. V. R. Cain, "A User's Manual for QAD-CG, the Combinatorial Geometry Version of the QAD-P5A Point Kernel Shielding Code", Bechtel Power Corporation(1977).
2. H. Ocken, "Radiation-Field Control Manual - 1997 Revision", TR-107991, Electric Power Research Institute(1997).
3. "Final Safety Analysis Report of Kori NPP #1", Korea Electric Power Company

4. Bernard Shlein, "The Health Physics and Radiological Health Handbook"(1992).
5. 송 명재, "방사선 피폭평가", 방사선-6, 한국전력공사 원자력연수원
6. "S/G Radiation Survey Sheet", Kori Unit #1 (1997).
7. James E. Turner, "Atoms, Radiation, and Radiation Protection", Mcgraw-HILL, INC., Health Profession Division(1985).
8. S. Shin, "Analysis of Cobalt Deposition Mechanisms in the Primary Coolant System of PWRs", TR-109006, Electric Power Research Institute(1997).